JOURNAL OF CATALYSIS **175,** 139–151 (1998)
ARTICLE NO. CA981984

Effects of Ethanol Impregnation on the Properties of Thoria-Promoted Co/SiO_2 Catalyst

Sui-Wen Ho[1]

Department of Chemistry, National Cheng Kung University, Tainan, Taiwan 701, Republic of China

Received May 12, 1997; revised December 3, 1997; accepted December 4, 1997

Two Th-added Co/SiO_2 catalysts were prepared by pore volume impregnation of 6 wt% Co_3O_4/SiO_2 with either aqueous or ethanol solutions. Smaller ThO_2 crystallites were obtained for the ethanol-prepared $Th/Co_3O_4/SiO_2$. The reduction behavior of cobalt oxide was modified by aqueous impregnation. Furthermore, Th addition was found to be promotional in the case of ethanol impregnation, or detrimental in the case of aqueous impregnation, for the CO oxidation activity of Co_3O_4/SiO_2. Th addition has no effect on the extent of reduction of cobalt phase, but (1) reduces the crystallite size of cobalt by hindering the sintering of cobalt metal; (2) increases the amount of hydrogen desorbed (150 or 190%), CO adsorbed (3 or 4 times), CO_2 evolved (2.6 or 4 times), and carbon deposited; (3) enhances the activity for CO disproportionation; (4) induces new CO adsorption modes, subcarbonyl-like species ($Co(CO)_x$, $x > 1$) and multifold CO ($(Co)_xCO$, $x \geq 2$); (5) decreases methanation activity; and (6) enhances the activity and the selectivity for higher hydrocarbons and olefins for Fischer–Tropsch synthesis. A roughening of the cobalt surface, which consists of steps and kinks induced by the decorated ThO_2 moieties around the interface area, is the proposed origin for the new adsorption and CO disproportionation sites. The more significant effects of Th addition when ethanol was employed as impregnation solvent instead of water is attributed to a more extensive $Co–ThO_2$ interface formed due to a better dispersed Th phase.

INTRODUCTION

Thoria has long been used as a promoter in Kieselguhr-supported cobalt catalysts for Fischer–Tropsch synthesis to increase the above C5 fraction and resist sulfur poisoning (1). The addition of Th was reported to affect the chemical and physical properties of the cobalt phase. Sexton *et al.* studied co-precipitated $Co–ThO_2$–Kieselguhr by temperature-programmed reduction and found that CoO was more resistant to reduction (2). However, Viwanathan *et al.* reported enhancement of the extent of reduction of cobalt and hydrogen adsorption for $Co–ThO_2$–Kieselguhr (3, 4). Rao *et al.* studied $Co–ThO_2$–ZSM-5 and found that thoria decreased the size of the cobalt particles and increased the synthesis gas conversion, the selectivity to gasoline range hydrocarbons, and the CO/H chemisorption ratio (5). Beuther *et al.* prepared thoria-promoted Co/Al_2O_3 catalyst with ethanol solution and reported high activity and selectivity for gasoline and diesel fuel hydrocarbons (6), but the nature of the ethanol effect is not clear. Although the effect of thoria on the catalytic properties of cobalt is well documented, previous studies were most performed on complicate systems with various cobalt phases and/or active supports. Furthermore, the influence of thoria on the adsorptive and desorptive properties of cobalt and their relationship to the catalytic properties has not been studied systematically.

In a previous study, we reported the preparation of silica-supported Co_3O_4, characteristic of complete reducibility and high dispersion (7). This material is well suited for the study of additive effect due to the simplicity of the system, i.e., fairly inert support and cobalt metal derived from mainly one kind of precursor without interference from unreduced cobalt phase that might complicate the interpretation of the observed activities and spectroscopic data. In order to systematically investigate the nature of Th promotion effect and the influence of ethanol impregnation, Th-added Co_3O_4/SiO_2 catalysts were prepared by sequential impregnation of Co_3O_4/SiO_2 with either ethanolic or aqueous solutions of thorium nitrate. The catalysts were characterized with X-ray diffraction, temperature-programmed analysis (TPR, TGA, TPD, TPSR), and infrared spectroscopy, and their activities for CO oxidation and CO hydrogenation were measured.

EXPERIMENTAL

Catalyst Preparation

The silica support (Cabol-O-Sil M5, BET surface area 190 m^2/g, pore volume 1.0 cm^3/g) was wetted, dried at 100°C for 16 h, calcined in air at 500°C for 10 min, and evacuated at 500°C for 1 h. Catalysts were prepared with incipient wetness impregnation performed under He flow (100 mL/min). The 6 wt% (as Co) Co_3O_4/SiO_2 was

[1] To whom correspondence should be addressed. Fax: 886-6-2740552. E-mail: rayho@mail.ncku.edu.tw.

0021-9517/98 $25.00

prepared by impregnation of the pretreated SiO_2 support with aqueous solution of cobalt nitrate (Alpha Products). The impregnated powders were dried at 120°C under He flow for 2 h, and calcined *in vacuo* at 300°C for 10 min. The cobalt phase in the as-prepared 6 wt% Co_3O_4/SiO_2 consists of 97% Co_3O_4 and 3% Co–SiO_4 interaction species (7). Th-added Co_3O_4/SiO_2 catalysts were prepared by impregnation of 6 wt% Co_3O_4/SiO_2 with either aqueous or ethanolic solutions of thorium nitrate (Alpha Products). The drying and calcination conditions were the same as that for 6 wt% Co_3O_4/SiO_2. The Th content was kept at the Th/Co atomic ratio of 0.5 (12.4 wt% ThO_2). The 6 wt% Co_3O_4/SiO_2, the aqua-prepared $Th/Co_3O_4/SiO_2$, and the ethanol-prepared $Th/Co_3O_4/SiO_2$ were abbreviated as Co/SiO_2, ThCoH, and ThCoE, respectively.

X-Ray Diffraction

X-ray powder diffraction patterns were obtained with a Shimadzu XD-D1 diffractometer equipped with a high-temperature cell. Powdered samples were packed into a $2 \times 0.5 \times 0.5$ cm^3 hollowed ceramic plate. The ASTM powder diffraction file was used to identify the phase presented. The crystallite sizes were calculated from line broadening using the Scherrer equation (8).

Infrared Spectroscopy

Infrared spectra were recorded on a Bomem MB 100, equipped with a DTGS detector and a quartz transmission cell. Samples of 30 mg were pressed into a 13 mm self-supported disc and loaded in the *in-situ* cell. After reduction at 400°C for 8 h in H_2 flow (50 mL/min), the cell was evacuated for 30 min ($<2 \times 10^{-6}$ Torr) at 400°C, then cooled to room temperature for CO adsorption. After CO adsorption (ca. 760 Torr for 1 h), the cell was evacuated for IR measurements. The raw spectra of the reduced sample were taken as reference.

Thermal Analysis

Temperature-programmed thermal analyses were performed on a Cahn TG-121 analyzer and/or a VG Sensorlab 300D mass spectrometer. In general, samples of 0.1–0.2 g were used. Temperature-programmed reduction was carried out under H_2 flow (50 mL/min) with a heating rate of 10°C/min to 400°C for 8 h. The extent of reduction of cobalt phase was measured based on the weight gain after re-oxidation of reduced sample at 400°C. For CO adsorption analyses, the sample was reduced first, further purged with He flow for 1 h to remove H_2, and then maintained at room temperature for CO adsorption. Carbon monoxide was introduced at a flow rate of 50 mL/min for a period of 1 h. Temperature-programmed desorption or hydrogenation was carried out under a He or H_2 flow, respectively, with a heating rate of 20°C/min.

Activity Measurements

Activity measurements were carried out in a flow microreactor consisting of Pyrex glass reactor (1/4 in.), stainless steel feed lines, temperature programmer (Watlow), and flow controller (Unit). For CO oxidation, the reactor was packed with 20 mg of catalyst on top of glass wool. A premixed CO/O_2/He (0.5/0.5/99, 99.999%, Scott) was introduced into the reactor at a flow rate of 50 mL/min at room temperature, and then the temperature was raised at a rate of 10°C/min to 150°C. The products were directly analyzed with a mass spectrometer. For CO hydrogenation, a 30 mg sample were used. After reduction, the temperature was maintained at 200°C. A premixed CO/H_2/He (3/9/88, 99.999%, Air Product) feed gas was introduced at a flow rate of 50 mL/min. The product was analyzed by gas chromatography using OV-101 and VZ-10 columns. For both reactions, the conversion of CO at steady state was below 5%.

RESULTS AND DISCUSSION

Effect of Ethanol Impregnation on Crystalline Phase

The X-ray diffraction patterns of the calcined 6 wt% Co/SiO_2 and Th-added Co/SiO_2, ThCoH and ThCoE, are given in Fig. 1a. Diffraction pattern characteristic of Co_3O_4 was observed for all samples. Same full width at maximum (FWHM) of Co_3O_4 ⟨311⟩ peak was obtained for all samples, and the crystallite size of Co_3O_4 based on the line broadening was ca. 130 Å. This clearly shows that sequential impregnation of the calcined 6 wt% Co/SiO_2 has little effects on the crystallite size of Co_3O_4. In addition, broad diffraction peaks of ThO_2 were observed for Th-added Co/SiO_2. In order to reveal the diffraction lines of ThO_2 clearly, the diffraction pattern of 6 wt% Co/SiO_2 was taken as background and was subtracted from that of Th-added Co/SiO_2. The resultant patterns are shown in Fig. 2. It can be seen that the diffraction lines of ThO_2 were much broader in ThCoE than in ThCoH, and the lines of ⟨111⟩ and ⟨200⟩ of ThO_2 were not resolved. This indicates that the Th phase is better dispersed when ethanol was employed as impregnation solvent. The FWHM of ThO_2 ⟨111⟩ line are 3.6 and 6.5°, corresponding to an average crystallite size of 23 and 13 Å for ThCoH and ThCoE, respectively. Smaller Co_3O_4 crystallites were obtained when ethanol was employed as an impregnation solvent instead of water and were attributed to the presence of ethoxyl groups which hindered the aggregation of cobalt oxide during calcination (7). The same mechanism may occur for thoria.

The X-ray diffraction patterns of reduced samples are shown in Fig. 1b. All diffraction lines of Co_3O_4 disappeared, and that of cobalt metal emerged for all reduced samples. Despite the same crystallite size of Co_3O_4 observed for the calcined samples, the FWHM of cobalt metal ⟨111⟩ line varied and were 0.68, 0.82, and 0.90°, corresponding to average

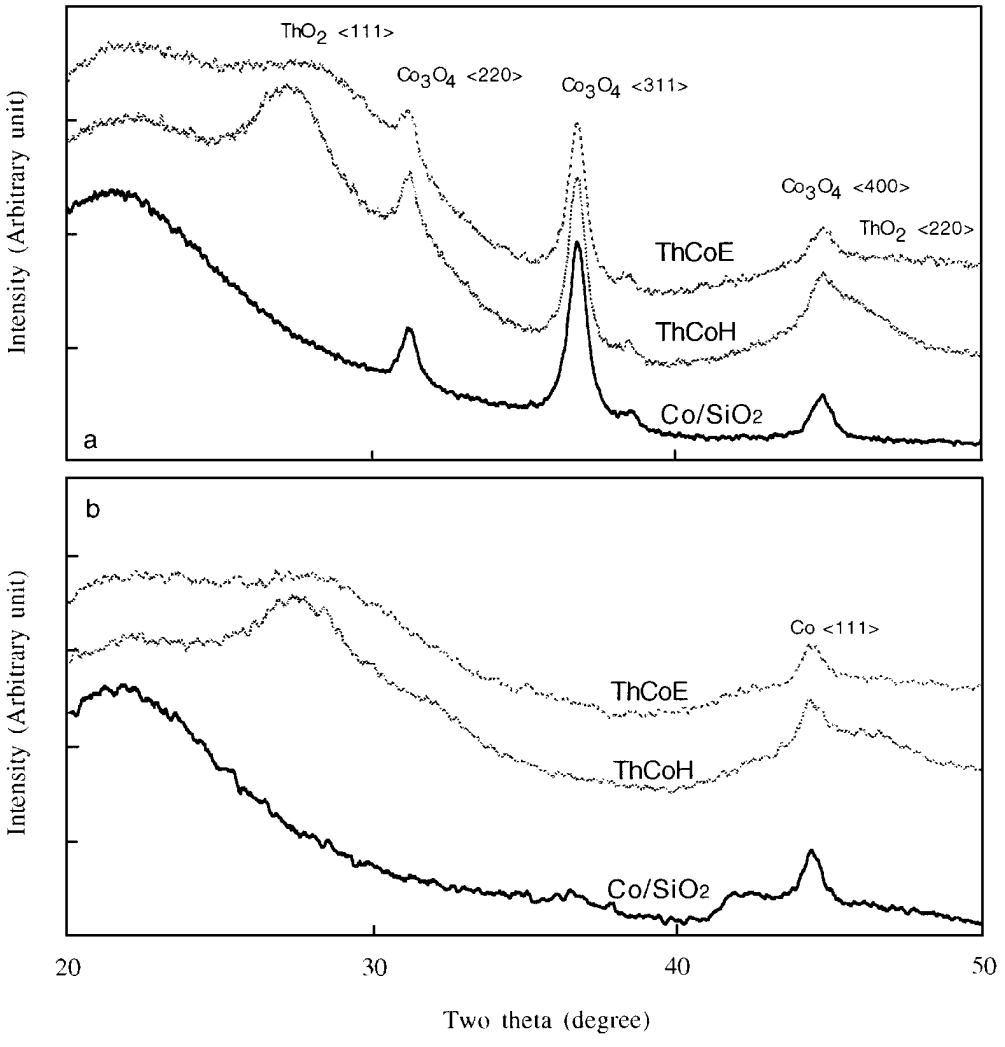

FIG. 1. X-ray diffraction patterns for 6 wt% Co/SiO_2, ThCoH, and ThCoE. (a) Catalysts as prepared. (b) Reduced catalysts.

crystallite sizes of 126, 107, and 95 Å, for Co/SiO_2, ThCoH, and ThCoE, respectively. The variation in the crystallite size of cobalt metal on Th addition may be rationalized by the influence of thoria on the sintering of cobalt metal during reduction treatment. Since thoria was better dispersed in ThCoE, the effect was greater, and consequently smaller Co crystallites were obtained. This explanation is consistent with early reports that thoria acted as structural modifier for cobalt catalysts (1, 5).

Th Effect on the Reduction Behavior of Cobalt Phase

The rates of weight losses as a function of temperature for the samples during temperature-programmed reduction are shown in Fig. 3. For 6 wt% Co/SiO_2, weight loss peaks located below 400°C corresponding to a two-stage reduction of Co_3O_4 and peak located at 530°C indicating a $Co–SiO_2$ interaction species were observed as reported previously (7). A similar TPR curve below 400°C but with larger and broader peaks at 530°C was obtained for ThCoE. The extra weight loss in the latter was attributed to the decomposition of the ethoxyl groups formed by ethanol on the silica surface (7). Therefore, impregnation of ethanolic Th solution was found to have no significant effect on the reduction behavior of cobalt phase. However, the 530°C peak was no longer present in the case of ThCoH. In addition, better resolved peaks representing the two-stage reduction of Co_3O_4 were observed. This indicates that the chemical property and the speciation of cobalt phase was modified by Th addition for the aqua-prepared $Th/Co/SiO_2$ and a more uniform Co_3O_4 phase was obtained. Haddad *et al.* studied the impact of aqueous impregnation on the calcined Co/SiO_2, and found that the reduction properties did not change after water impregnation (9). It was reported that the formation of $Co–SiO_2$ interaction species is favored when pH of the impregnation solution is above 5 (10, 11). This may be due to the creation of negatively charged sites, $\sim Si–O^-$, which interact with positive Co(II) ions to form the surface Co

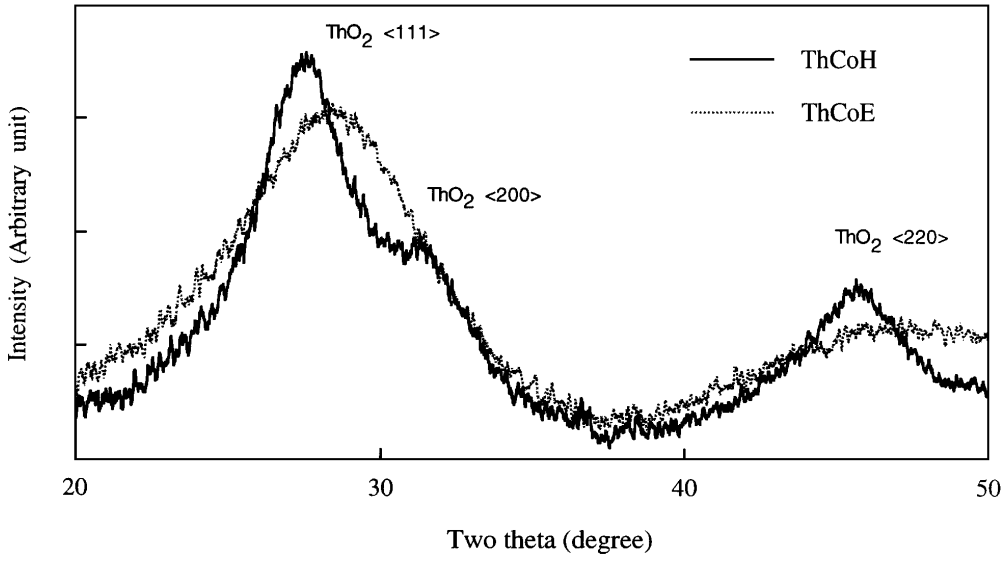

FIG. 2. X-ray diffraction peaks of ThO_2 phase in ThCoH and ThCoE. The peaks were obtained by subtracting the diffraction pattern of 6 wt% Co/SiO_2 from those of ThCoH and ThCoE.

species. Due to the hydrolysis of water by Th(IV) ion, the aqueous solution of thorium nitrate is quite acidic and the pH value (ca. 1) is comparable to the isoelectric point of silica (pH 1–2) (12); as a consequence, the Co–SiO_2 interaction species might no longer be stable, cobalt ion redissolved was deposited on Co_3O_4 crystallites during drying and transformed into Co_3O_4 in the calcination step.

Sexton *et al.* reported a resistance of reduction on the second reduction stage ($CoO \rightarrow Co$) during temperature-programmed reduction when cobalt–Kieselguhr catalysts was promoted with ThO_2, and a solid–solution phase of $CoO–ThO_2$ was suggested (2). This phenomena was not observed on our sequentially prepared $Th/Co/SiO_2$ excluding strong interaction between added ThO_2 phase and Co_3O_4 phase. The different behavior may be due to the different preparation method; co-precipitation with excess base was employed by Sexton *et al.*, a process known to form mixed precipitates. The inhibition of cobalt reduction by ThO_2 may be due to physical barrier, such as diffusion of water produced (13), instead of the proposed chemical interaction between CoO and ThO_2. One important point here is that the cobalt phase was not buried by ThO_2 in the sequentially prepared catalysts, ThCoH and ThCoE.

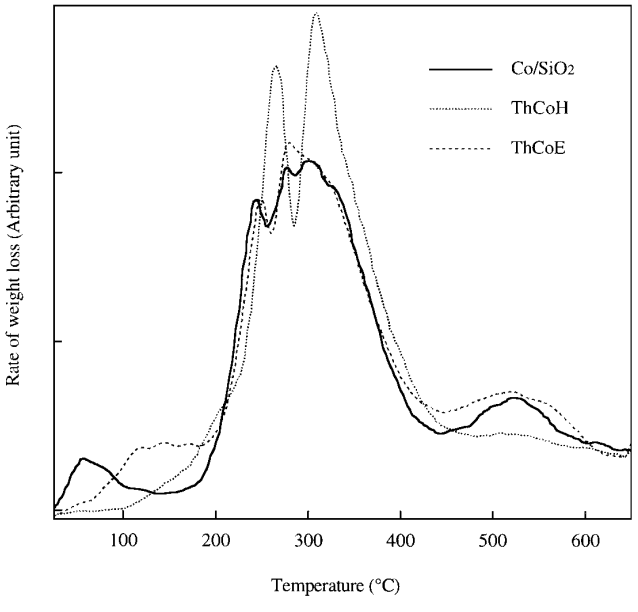

FIG. 3. DTG curves of the catalysts obtained in temperature-programmed reduction.

Solvent Effect on CO Oxidation Activity

Cobalt oxide, especially Co_3O_4, is known to be very active in catalyzing CO oxidation (14). The influence of solvent on the Th effect was further probed by measuring the activity of the calcined catalysts in catalyzing CO oxidation. The rates of CO oxidation versus time on stream are shown in Fig. 4. Similar trend of rate decay was observed for 6 wt% Co/SiO_2 and ThCoE. The sharp decline of activity in initial period was attributed to the deposition of carbon from CO disproportionation (15). The similar decay trend indicates similar kinds of active sites were present on the two catalysts. For ThCoH, after initial activity drop, the rate increased slightly and reached steady state after 3 h. The different activity behavior between 6 wt% Co/SiO_2 and ThCoH indicates the modification of surface properties of Co_3O_4 by sequential impregnation of aqueous thorium nitrate solution. It is worth mentioning that the influence of Th addition on the catalytic behavior of Co_3O_4/SiO_2 for CO oxidation correlated with the results of TPR. The steady state rates were modified on Th addition, and were 1.2×10^{-5} (2.3%

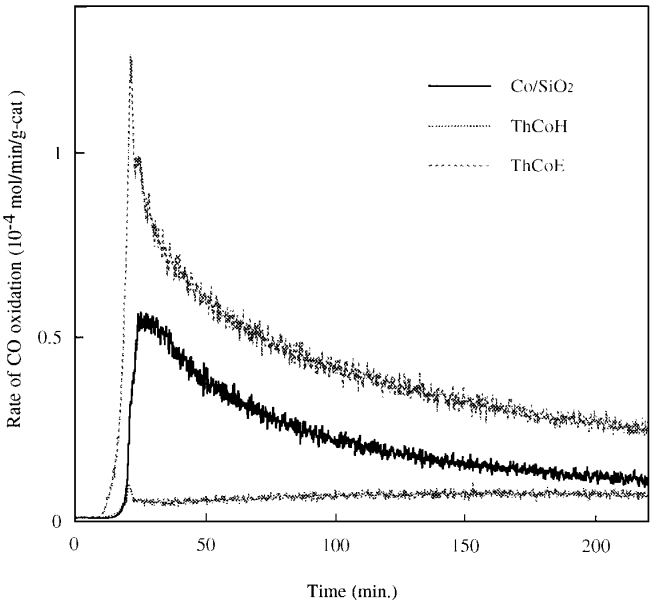

FIG. 4. Activities of the catalysts for CO oxidation as a function of time on stream.

conversion), 8.6×10^{-6} (1.4%), and 2.6×10^{-5} (4.2%) mol/min/g-cat for 6 wt% Co/SiO_2, ThCoH, ThCoE, respectively. In a previous study, an increase in CO oxidation activity of Co_3O_4/SiO_2 was found when ethanol was employed as impregnation solvent (15) and was attributed to the modified Co_3O_4 surface by the carboneous species derived from ethanol. The decreased activity for ThCoH may be related to the modified surface structure of Co_3O_4 as indicated by TPR. Another factor, decrease in the surface area due to the covering of active Co_3O_4 surface by ThO_2 patches, is more likely to occur in ThCoH than in ThCoE, since the Th phase is better dispersed in ThCoE.

Th Effect on the Adsorption Mode of CO

After exposure of the reduced pellet to ca. 760 Torr of CO for 1 h at room temperature (RT), the cell was evacuated for another 1 h before IR measurement. The absorbance spectra of adsorbed CO for the reduced catalysts are shown in Fig. 5. For 6 wt% Co/SiO_2, an intense peak at 2011 cm^{-1} with two weak shoulders at 2068 and 1935 cm^{-1} was observed. The 2011 cm^{-1} peak can be readily assigned to CO adsorbed on cobalt metal in linear geometry (16–19). The 2068 cm^{-1} shoulder can be assigned to the surface carbonyl species, $Co(CO)_x$ (where $x > 1$) (19–20), and the 1935 cm^{-1} shoulder to the bridged CO. For Th-added Co/SiO_2, the absorbance in the 2000 cm^{-1} region increased significantly, and two additional bands at 1816 and 1610 cm^{-1} appeared. The 1816 cm^{-1} band was assigned to the CO adsorbed on multifold sites (21). On the basis of a broad absorption band between 1300 and 1750 cm^{-1}, Kip *et al.* proposed the

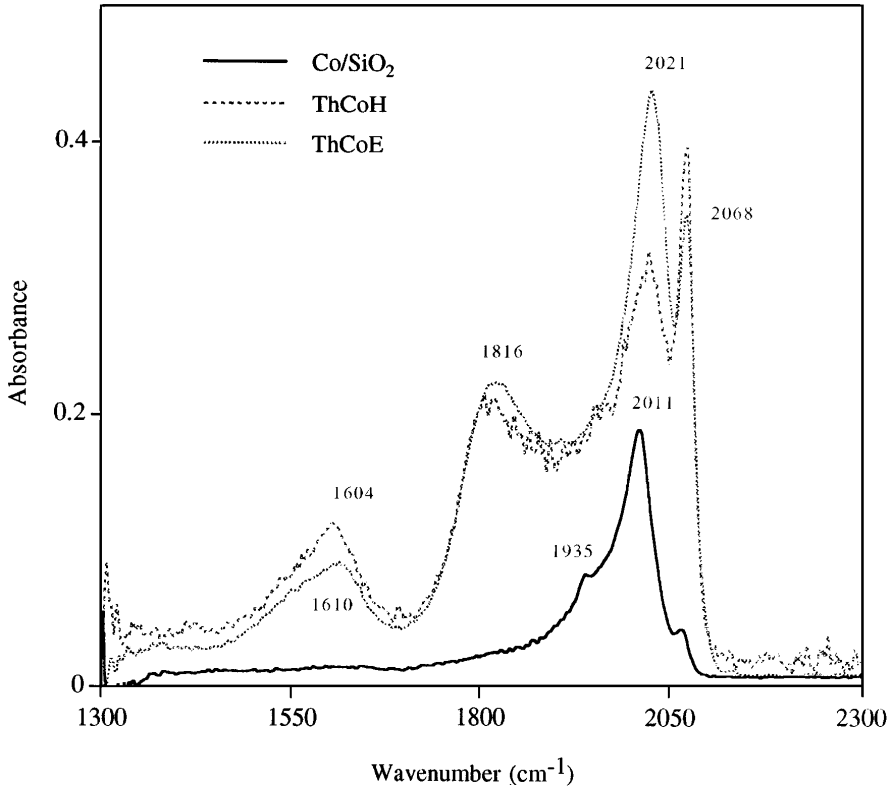

FIG. 5. Absorbance spectra of CO adsorbed at RT for catalysts reduced at 400°C for 8 h.

"side-bonded" CO on the Co–ThO_2 interface, with its carbon atom to the metal and its oxygen atom to the ThO_2, as the active species for CO dissociation (22). The broad band at 1610 cm^{-1} for Th-added Co/SiO_2 is within the reported region, however, this band was assigned to carbonate species on ThO_2 surface because the same band was detected for silica-supported thoria when exposed to CO at the same conditions as that for Th-added Co/SiO_2 (23). It is suspected that the 1300–1750 cm^{-1} band reported by Kip *et al.* may be carbonate species on thoria surface instead of "side-bonded" CO. Clearly, the CO adsorption mode on cobalt surface was dramatically modified in the presence of thoria, and the relative amount of CO adsorption mode depends on the solvent employed for Th impregnation. This also indicates the existence of intimate contact of Th phase with cobalt, possibly via decoration of cobalt surface by some ThO_2 moieties.

Th Effect on the Desorption Behavior of H_2

After reduction at 400°C for 8 h, the catalysts were cooled to RT in hydrogen for 1 h, exposed to He, and temperature programmed to 400°C to desorb hydrogen. The TPD spectra are shown in Fig. 6. A single desorption peak located at 120°C with a tail extended to 300°C was observed for 6 wt% Co/SiO_2. The observed desorption temperature of 120°C is consistent with the temperature reported for hydrogen desorbing from unsupported cobalt metal (24, 25), and was assigned to the hydrogen desorbed directly from cobalt metal surface. This indicates that the chemisorptive properties of cobalt was not affected by the silica support in the prepared 6 wt% Co/SiO_2 as it was planned to be. The tailing feature may be due to the spillover hydrogen. For Th-added Co/SiO_2, the total amount of desorbed hydrogen increased, 150 and 190% as compared to that of Co/SiO_2 for ThCoH and ThCoE, respectively. The intensity of the hydrogen desorption band at 120°C is lower for Th-added catalysts as shown by the difference spectra in Fig. 7. This may due to the partial covering of cobalt surface by ThO_2. The extra hydrogen was mainly desorbed over a temperature range of 150–300°C, and the increase in the amount of desorbed hydrogen cannot be fully accounted by the decrease in cobalt crystallite size on Th addition estimated by XRD line broadening. The exact location of the extra hydrogen is not clear. A number of possibilities exist, such as the creation of new adsorption sites for hydrogen on the Co–ThO_2 interface, the spillover hydrogen onto the surface of ThO_2, or adsorption sites on a roughened cobalt surface induced by ThO_2 decoration.

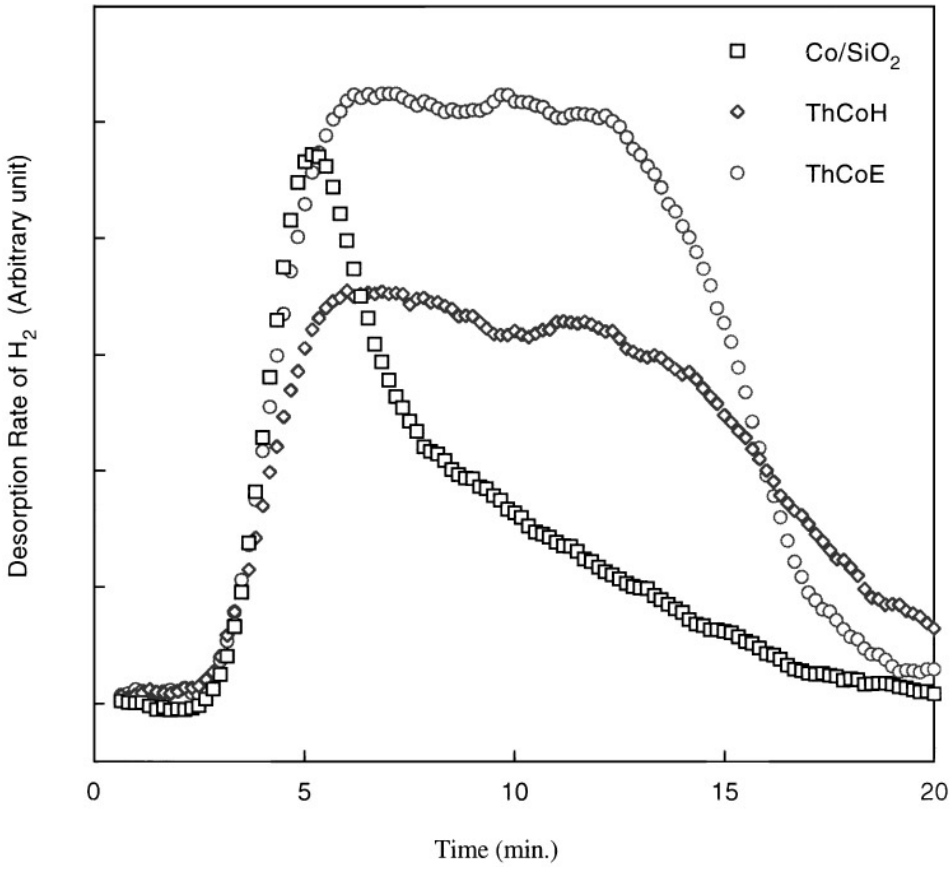

FIG. 6. TPD spectra of hydrogen desorption following activated adsorption of hydrogen at 400°C on the catalysts reduced at 400°C for 8 h.

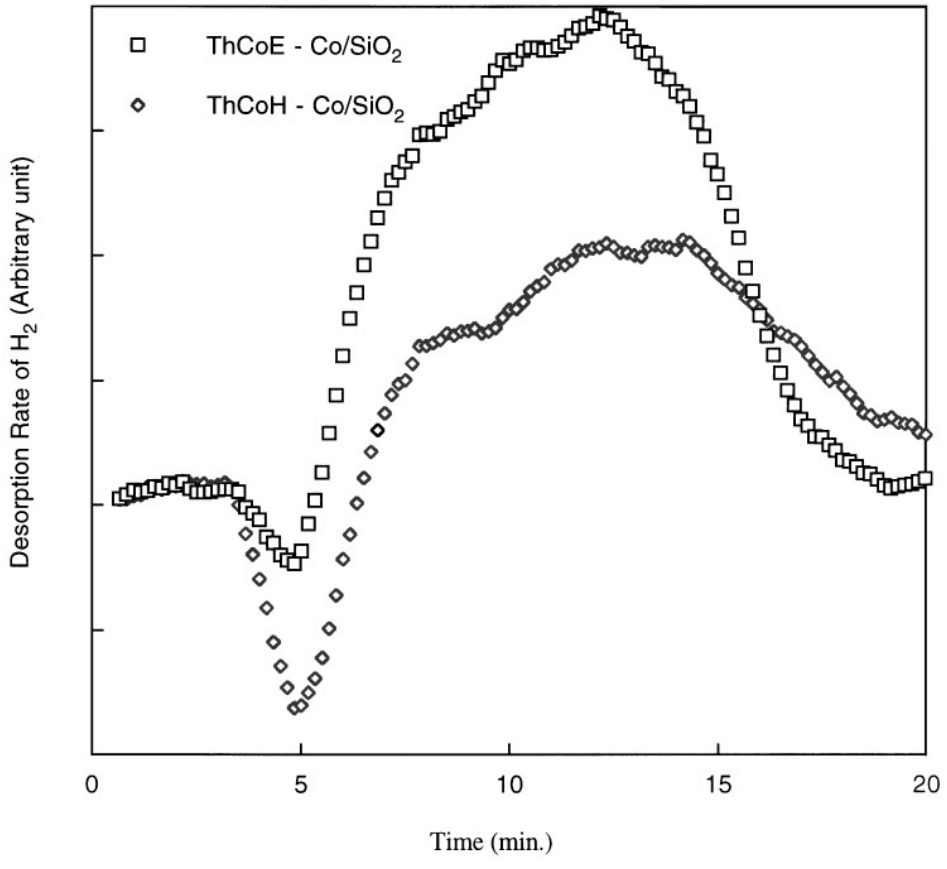

FIG. 7. Difference TPD spectra of hydrogen desorption between that for Th-added catalysts and 6 wt% Co/SiO_2.

Th Effect on the Desorption Behavior of CO

The TPD spectra for CO desorption following adsorption of CO at RT on the reduced catalysts are shown in Fig. 8. A single band located at 130°C was observed for 6 wt% Co/SiO_2. This is comparable to the reported desorption temperature of CO from polycrystalline Co and Co(0001) surface (157–147°C) (26, 27), and Co(1012) (97°C) (28). For Th-added Co/SiO_2, an additional intense band at 170–180°C appeared, and the total amount of desorbed CO increased two and five times that of 6 wt% Co/SiO_2 for ThCoH and ThCoE, respectively. In addition to CO desorption, CO_2 was also detected during temperature-programmed treatment by mass spectrometer. The TPD spectra of CO_2 are shown in Fig. 9. Two peaks located at 200 and 285°C were found for 6 wt% Co/SiO_2. For Th-added Co/SiO_2, desorption of CO_2 occurred below 100°C, and desorption bands located at 150, 230, and 270°C were observed for both ThCoH and ThCoE. Additional CO_2 desorption around 350°C was found for ThCoE. The total amount of CO_2 desorption also increased to 2.6 and 4 times that of Co/SiO_2 for ThCoH and ThCoE, respectively.

The quantitative result of CO adsorption and desorption by thermogravimetric analysis–mass spectroscopy are given in Table 1. For 6 wt% Co/SiO_2, the weight gain is 0.14% for CO adsorption at RT, and the weight loss for temperature-programmed desorption to 400°C is 0.096%, resulting in a residue weight of 0.04%. For Th-added Co/SiO_2, more weight gain due to CO adsorption was obtained, i.e. 0.41 and 0.50% for ThCoH and ThCoE, respectively. After

TABLE 1

Weight Changes of CO Adsorption and Desorption Obtained by Thermogravimetric Analysis–Mass Spectroscopy

Treatments	6 wt% Co/SiO_2	ThCoH	ThCoE
Wt gain (%), adsor.	0.14	0.41	0.50
Amt. of CO (μmol)[a]	49	144	177
Wt loss (%), TPD	0.096	0.30	0.37
Wt loss (%), TPD–MS[b]	0.098	0.28	0.42
Amt. of CO (μmol)[a]	10	20	48
Amt. of CO_2 (μmol)[a]	16	41	65
Residue wt (%)	0.04	0.09	0.10
Amt. of C (μmol C)[c]	34	71	83

[a] Amount of CO or CO_2 per gram 6 wt% Co/SiO_2 (excluding the weight of thoria).

[b] The weight loss calculated from the amount of CO and CO_2 desorbed. Weight loss = (28 × moles of CO) + (44 × moles of CO_2).

[c] The amount of deposited carbon calculated from the residue weight assuming carbon is the only carbon species after TPD.

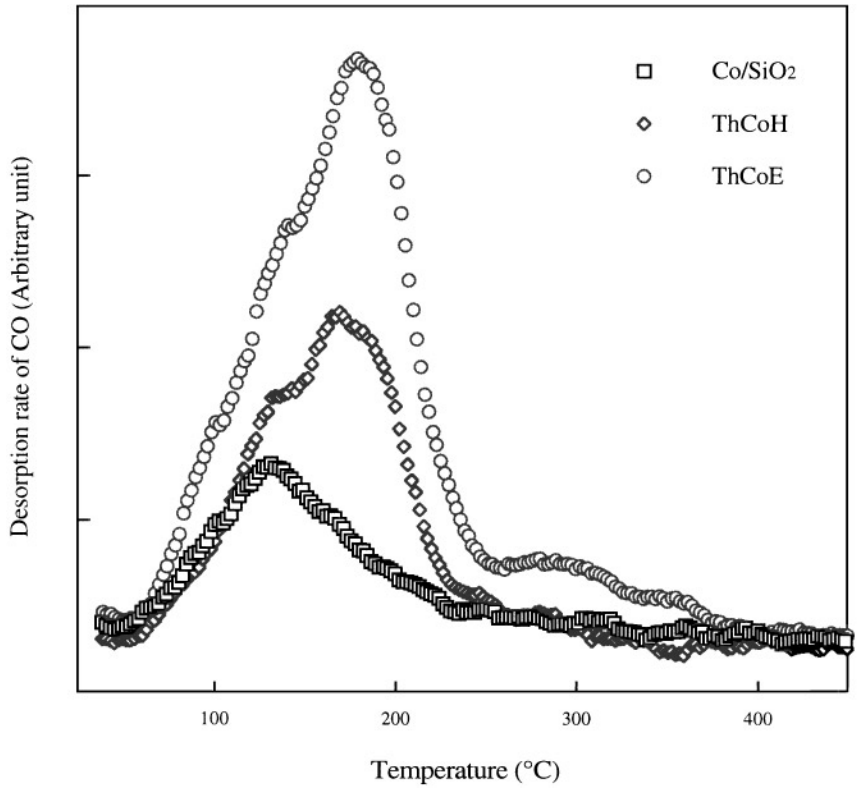

FIG. 8. TPD spectra of CO desorption following adsorption of CO at RT on the catalysts.

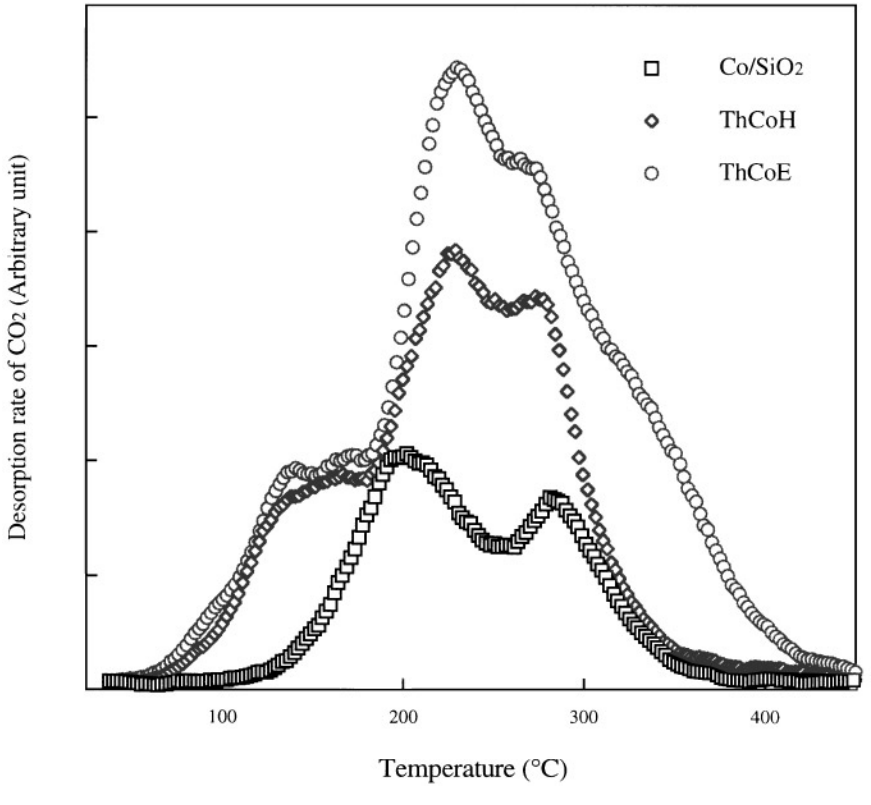

FIG. 9. TPD spectra of CO_2 desorption following adsorption of CO at RT on the catalysts.

temperature-programmed desorption, residue weights 0.09 and 0.10% were also obtained. The weight loss during desorption can also be estimated from the number of mole of desorbed CO and CO_2 determined by mass spectroscopy. A value of 0.098% which agrees well with that (0.096%) determined from thermogravimetric analysis was obtained. The same calculations were applied to ThCoH and ThCoE, and a good agreement is also obtained (see Table 1). The agreements indicate that the weight loss is totally due to the desorption of carbon species, CO and CO_2.

When the reduced 6 wt% Co/SiO_2 was exposed to CO at RT, gas phase CO_2 was detected by IR indicating the occurrence of CO disproportionation. Niemela *et al.* also reported CO_2 formation during CO pulsing at RT on Co/SiO_2 (29). After evacuation, gas phase CO_2 was completely removed, and no bands characteristic of CO_2 adsorbed on cobalt were detected by IR. Therefore, the desorbed CO_2 during TPD cannot be attributed to the chemisorbed CO_2. Clearly, the temperature-programmed desorption of CO from Co/SiO_2 is a complicated process involving other reactions such as CO dissociation (26) and CO disproportionation. It is likely that the 200°C peak of CO_2 desorption resulted from CO disproportionation (30), and the 285°C from the recombination of dissociated carbon and oxygen (26) for 6 wt% Co/SiO_2. The additional 150°C desorption band for ThCoH and ThCoE suggests the presence of more active sites for CO disproportionation on Th addition. Assuming that the residue weight was due to the deposited carbon from CO disproportionation, 34 μmol of carbon per gram of 6 wt% Co/SiO_2 was obtained. It is larger than the amount (16 μmol/g-Co/SiO_2) of CO_2 desorbed. Larger values were also obtained for ThCoH and ThCoE (Table 1). This indicates the existence of other contributions, such as adsorbed oxygen or carbon produced from CO dissociation during CO adsorption at RT. The percentage of CO_2 desorbed for Co/SiO_2 is 61.5%, which is unusually high compared to other group VIII metals, such as Ni (31, 32), Rh (33–35), and Fe (36). The high activity of cobalt for CO disproportionation may be relevant to the catalytic behavior of cobalt in production of higher hydrocarbons in Fischer–Tropsch synthesis.

The amount of CO adsorption was increased 3 or 4 times on Th addition (Table 1), new adsorption sites must be created to accommodate more CO. One way is to increase the cobalt surface area, for example, by roughening of the cobalt surface induced by the decorated ThO_2 moieties around the interface area. The roughened surface may contain more steps and kinks and, therefore, may chemisorb more hydrogen strongly or favor the formation of subcarbonyl-like species and multibonded CO, as detected by IR. Since CO dissociation on cobalt was reported to be structure sensitive, the stepped (1012) and the zigzag, grooved (1120) surfaces are active (27, 37, 38), while the smooth (0001) is not (25). Therefore, the proposed roughness of cobalt surface may also provide an explanation to the observed increase of the activity for CO_2 formation (Fig. 9 and Table 1) via CO disproportionation. The other possibility is the adsorption sites on ThO_2 surface. A number of species, such as adsorbed CO, carbonates, and formates, were reported to form on the surface of thoria (39). The presence of adsorbed CO (2067 and 1873 cm^{-1}) and carbonates (1610 cm^{-1}) was detected by IR, as well as the release of CO and CO_2 during temperature-programmed desorption after silica-supported thoria was exposed to CO at RT (23). It is expected that the amount of CO adsorption on thoria may increase in the presence of Co metal via spillover.

The effects of Th addition on the adsorption and desorption properties of CO is more significant when ethanol was employed as impregnation solvent instead of water. This can be rationalized by the highly dispersed ThO_2 phase for the ethanol-prepared $Th/Co/SiO_2$ catalysts, which means higher ThO_2 surface area, and therefore more Co–ThO_2 interface for CO adsorption and CO disproportionation.

Reactivity of Deposited Carbon and Adsorbed CO

The reactivity of residue carbon after desorption treatment at 400°C was studied by temperature-programmed hydrogenation. Methane was detected by mass spectrometer. The rate of methane formation versus temperature is shown in Fig. 10. Methane formation was found above 200°C, and the major formation peaks were located at 220, 250, and 240°C for Co/SiO_2, ThCoH, and ThCoE, respectively. These values are close to the reported temperature (190°C) for methane peak of atomic carbon ($C\alpha$) deposited on Co/Al_2O_3 through CO disproportionation at 250–400°C (40). The higher temperature for Th-added catalysts indicates the lower reactivity of deposited carbon on these catalysts in methane formation.

The reactivity of carbon species after CO adsorption at RT was also studied by temperature-programmed hydrogenation. The rate of methane formation as a function of temperature was shown in Fig. 11. Methane formation began at 120°C and was nearly complete before 220°C. Higher methanation rate was found for 6 wt% Co/SiO_2 below 150°C. The temperature of the maximum methanation rate is 158°C for Co/SiO_2, which agrees well with the reported 154°C for unsupported metal (41). Slightly higher temperatures of 169 and 186°C were observed for ThCoH and ThCoE, respectively. It is worth mentioning that the reactivity of the absorbed CO species is higher than that of the deposited carbon for all catalysts. The rate of ethane formation versus temperature is shown in Fig. 11. Ethane was barely observable for 6 wt% Co/SiO_2, but was found to form in the same temperature range as for methane formation for ThCoH and ThCoE. Similar patterns as that of ethane were obtained for propane. This indicates that carbon chain growth was promoted by Th addition.

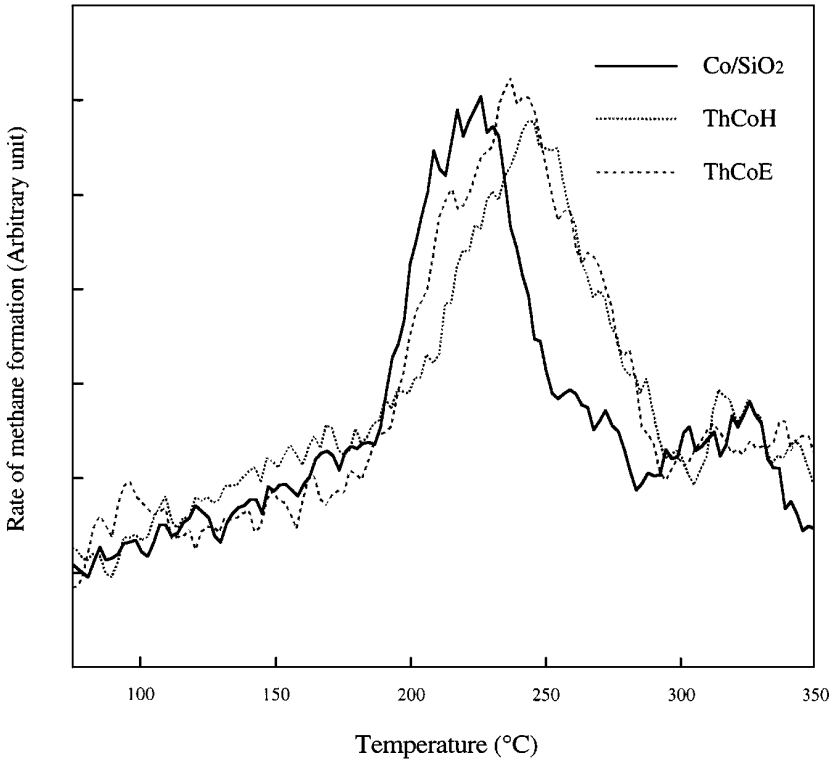

FIG. 10. Reactivity of residue carbon species measured by temperature-programmed hydrogenation for the catalysts.

Th Effect on the Activity and Selectivity of CO Hydrogenation

The results of activity measurement are given in Table 2. It can be seen that the steady state activity increased from 21.2 mmol/g of Co/h for 6 wt% Co/SiO_2 to 29.2 and 52.8 mmol/g of Co/h for ThCoH and ThCoE. The TOF's are 4.4×10^{-3}, 2.9×10^{-3}, and $6.9 \times 10^{-3}\,s^{-1}$ for 6 wt% Co/SiO_2 based on the cobalt dispersion estimated from the results of XRD, H_2 desorption (assuming $H_{des}/Co_{surf} = 1$), and CO

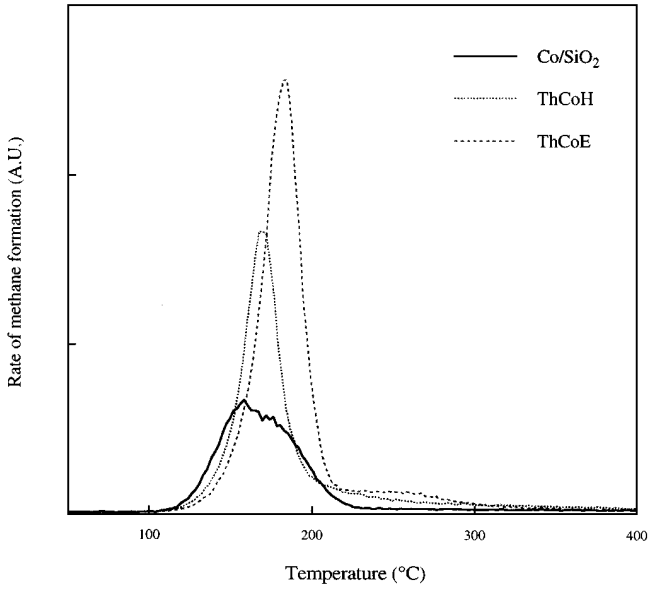

FIG. 11. Rates of methane formation during temperature-programmed hydrogenation for the catalysts after CO adsorbed at RT.

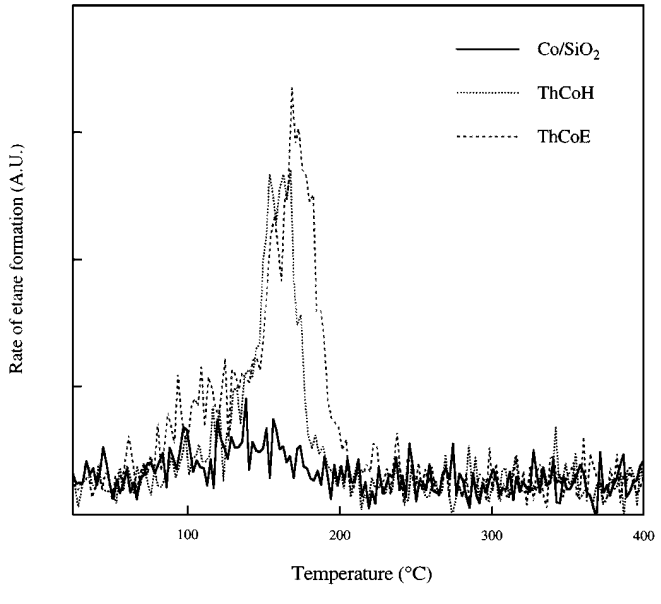

FIG. 12. Rates of ethane formation during temperature-programmed hydrogenation for the catalysts after CO adsorbed at RT.

TABLE 2

CO Hydrogenation Activities and Selectivities at Reaction Temperature of 200°C

Catalyst	Activity (mmol/g of Co/h)		TOF (10^{-3} s^{-1})[c]			Selectivity (%)						Olefin to paraffin ratio		
	C_T[a]	C1[b]	XRD	H_2	CO	C1	C2	C3	C4	C2–C4	$C5^+$	C2	C3	C4
Co/SiO_2	21.2 (1.0%)	9.9	4.4 (7.9)	2.9 (12)	6.7 (5.2)	48	9	19	10	38	14	0.5	5.8	3.6
ThCoH	29.2 (1.2%)	4.7	9.3 (9.3)	2.7 (17)	3.1 (15)	18	5	13	13	31	51	4.9	26.3	15.1
ThCoE	52.8 (2.1%)	9.2	11 (11)	3.9 (22)	4.6 (19)	19	5	15	14	34	47	1.9	17.1	8.1

[a] Activity of steady state in number of CO transformed into hydrocarbons. The numbers in parentheses are CO conversions under the experimental conditions.

[b] Activity of steady state in number of CO transformed into methane.

[c] Turnover frequencies based on cobalt dispersion (values in parentheses) estimated from the results of XRD, hydrogen desorption, and CO chemisorption. Assuming an adsorption stoichiometry of $H_{des}/Co_{surf} = 1$ and $CO_{ad}/Co_{surf} = 1$.

chemisorption (assuming $CO_{ad}/Co_{surf} = 1$) respectively. The value of 2.9×10^{-3} s^{-1} for 6 wt% Co/SiO_2 is in agreement with the previous studies (15, 42). For example, the data of Reuel and Bartholomew extrapolated to 200°C give TOF values of 2.6×10^{-3} and 3.1×10^{-3} s^{-1}, respectively, for 3 and 10% Co/SiO_2 (42). The activation energies of about 69 kJ/mol for CO conversion and 114 kJ/mol for methanation are in reasonable agreement with previous work (42–44) but agree most closely with the values reported for a 3% Co/SiO_2 catalyst (42). Higher TOF values from CO uptake (43, 44) and XRD are obviously due to an underestimation of cobalt dispersion. The variation of TOF on Th addition is dependent on how cobalt dispersion was obtained. Both ThCoH and ThCoE give lower TOF values as compared to that of 6 wt% Co/SiO_2 when cobalt dispersion was obtained from CO uptake. This may be attributed to an overestimation of the relative surface cobalt atom, since a significant amount of CO is found to be adsorbed on thoria surface as indicated by IR. On the other hand, an enhancement in TOF based on XRD to ca. twice and 115% for CoThE and CoThH, respectively, is obtained. An increment in surface area due to roughness caused by Th decoration cannot be detected by XRD, therefore, an overestimation of the enhancement in TOF on Th addition may occur. A fraction of desorbed hydrogen originated from the spillover hydrogen as indicated by the TPD curves, hence, higher TOF's than the values presented in Table 2 for ThCoH and ThCoE are expected. Consequently, the percentage of increase in TOF on Th addition is expected to be within that estimated from XRD and H_2 desorption. In conclusion, Th addition has a moderate effect on the turnover frequency, and the higher activity on a per gram of cobalt basis observed on Th addition may be largely due to the increase cobalt surface are induced by Th decoration, and partly to more active sites induced in that area.

The methane selectivities decreased to a similar extent (from 48 to 18 or 19%) for both Th-added catalysts. The selectivity for hydrocarbons with carbon number larger or equal to 5 ($C5^+$) increased for Th-added catalysts as reported (1, 5). Similar selectivities for C2, C3, C5, and $C5^+$ are obtained for ThCoH and ThCoE as well. More olefins in C2–C4 fraction were produced on Th addition as indicated by the increased olefin to paraffin ratio; however, more olefins were formed for the aqua-prepared $Th/Co/SiO_2$. The decreased methane selectivity is directly related to the lower hydrogenation activity as indicated by temperature programmed hydrogenation, which decreased the rate of the chain-terminating steps and is attributed to the electronic donation of decorated ThO_2 to cobalt (5, 36, 45). The increased activity of CO disproportionation caused an increase in the surface concentration of carboneous species, facilitated the carbon chain growth, and hence favored the formation of higher hydrocarbons. Despite the lower hydrogenation ability, the higher rate of carbon chain growth resulted in higher CO conversion to hydrocarbons. The similar selectivity for the two Th-added catalysts indicates same kind of active sites. Therefore, the higher activity for ThCoE is attributed to the more $Co–ThO_2$ interface due to the better dispersed Th phase and less blocking of cobalt surface. The lower olefin to paraffin ratio for ThCoE may due to the higher conversion under which secondary reaction proceeded to a more extent.

CONCLUSIONS

The chemical states and catalytic properties of Th-added Co_3O_4/SiO_2 catalysts depend on the solvent used for sequential impregnation. The results of X-ray diffraction show that the average crystallite size of Co_3O_4 remains unchanged, and smaller ThO_2 crystallites are obtained when

ethanol is employed as impregnation solvent instead of water. This is attributed to the presence of ethoxyl groups which hindered the aggregation of ThO_2 during calcination. However, temperature-programmed reduction indicates that the Co–SiO_2 surface species disappear, and a more uniform Co_3O_4 phase is present in the aqua-prepared $Th/Co_3O_4/SiO_2$ catalyst. The effect of Th addition on the CO oxidation activity depends on the impregnation solvent, and is found to be either promotional in the case of the ethanol-prepared $Th/Co_3O_4/SiO_2$ or detrimental in the case of the aqua-prepared one.

Th addition has no effect on the extent of reduction of cobalt phase, and cobalt phase is completely reduced into cobalt metal after reduction treatment at 400°C for 8 h. The average size of cobalt crystallite decreases on Th addition due to the hindering of cobalt sintering by thoria. Since thoria is better dispersed in the ethanol-prepared $Th/Co/SiO_2$, the effect is more significant. The amount of desorbed hydrogen increases to 150 or 190% on Th addition. The increment cannot be fully accounted for by the decrease in cobalt crystallite size, therefore, is attributed to the hydrogen adsorbed on the Co–ThO_2 interface and the spillover hydrogen on the ThO_2 surface. The amount of adsorbed CO increases 3 or 4 times on Th addition, and the adsorption mode is modified as well. In addition to terminal CO, which is the major CO species on 6 wt% Co/SiO_2, subcarbonyl-like species ($(Co(CO)_x$, $x > 1$) and multifold CO ($((Co)_xCO$, $x \geq 2$) are present. A roughened cobalt surface which consists of steps and kinks induced by the decorated ThO_2 moieties around the interface area is proposed for the new adsorption sites. Carbonates formed on ThO_2 surface and CO_2 in gas phase are detected on CO adsorption. CO_2 is a product of CO disproportionation, hence, corresponding amount of carbon is deposited on the cobalt surface. Terminal CO was also observed on ThO_2 surface for silica supported thoria. All the above mentioned carbon species contributed to the CO adsorption on the Th-added Co/SiO_2. During temperature-programmed desorption, CO and CO_2 were detected for all catalysts, the former mainly desorbed below 200°C and the latter above 200°C. The amount of desorbed CO_2 is always higher than that of desorbed CO indicating that cobalt is very active for CO disproportionation. Th addition increases both the amount of desorbed CO and CO_2, and the increment is larger for the ethanol-prepared $Th/Co/SiO_2$. In addition, the formation of CO_2 was occurred at lower temperature (<100°C). This indicates the creation of active sites for CO disproportionation, possibly at the Co–ThO_2 interface area.

Methane was observed above 200°C during temperature-programmed hydrogenation of deposited carbon, and higher temperature was observed for Th-added catalysts indicating the decreased activity for methanation on Th addition. The decreased activity for methanation on Th addition was also observed for CO adsorbed at RT. This is consistent with the observed decrease in methane selectivity from 48 to 18 or 19% on Th addition, reflecting the decreased activity of hydrogenation due to the electron-donating effect of decorated ThO_2 on cobalt metal. Despite the decrease in hydrogenation activity on Th addition, the CO conversion to hydrocarbons actually increased because of the enhanced growth of carbon chain by the higher surface density of carbon species derived from CO disproportionation, hence, the enhanced selectivities for higher hydrocarbons and olefins were obtained.

The effects of Th addition were generally found to be more significant when ethanol was employed as impregnation solvent instead of water. This is attributed to the more Co–ThO_2 interface formed and less blocking of cobalt surface by the decorated ThO_2 moieties due to the better dispersed Th phase.

ACKNOWLEDGMENTS

This work was supported by the National Science Council, Republic of China.

REFERENCES

1. Storch, H. H., Golumbic, N., and Anderson, R. B., "The Fischer–Tropsch and Related Synthesis." Wiley, New York, 1951.
2. Sexton, B. A., Hughes, A. E., and Turney, T. W., *J. Catal.* **97**, 390 (1986).
3. Viswanathan, B. J., and Gopalakrishnan, R., *J. Catal.* **99**, 342 (1986).
4. Gopalakrishnan, R., and Viswanathan, B., *J. Chem. Soc., Faraday Trans. 1* **82**, 2635 (1986).
5. Rao, V. U. S., Gormley, R. J., Shamsi, A., Peterick, T. R., Stencel, J. M., Schehl, R. R., Chi, R. D. H., and Obermyer, R. T., *J. Mol. Catal.* **29**, 271 (1985).
6. Beuther, H., Kibby, C. L., Kobylinski, T. P., and Pannel, R. B., U.S. Patent 4,605,680, 1986.
7. Ho, S. W., and Su, Y. S., *J. Cata.* **168**, 51 (1997).
8. Klug, H. P., and Alexander, L. E., "X-ray Diffraction Procedures," p. 491. Wiley, New York, 1954.
9. Haddad, G. J., and Goodwin, J. G., Jr., *J. Catal.* **157**, 25 (1995).
10. van Steen, E., Sewell, G. S., Makhothe, R. A., Micklethwaite, C., Manstein, H., de Lange, M., and O'Connor, C. T., *J. Catal.* **162**, 220 (1996).
11. Ming, H., and Baker, B. G., *Appl. Catal.* **123**, 23 (1995).
12. Parks, G. A., *Chem. Rev.* **65**, 177 (1965).
13. Castner, D. G., Watson, P. R., and Chan, I. Y., *J. Phys. Chem.* **94**, 819 (1990).
14. Boreskov, G. K., *in* "Catalysis, Science and Technology" (J. R. Anderson and M. Boudart, Eds.), Vol. 3, p. 39. Springer, Berlin, 1982.
15. Ho, S. W., and Su, Y. S., *J. Chin. Chem. Soc.* **44**, 1 (1997).
16. Mohana Rao, K., Spoto, G., and Zecchina, A., *J. Catal.* **113**, 466 (1988).
17. Sato, K., Inoue, Y., Kojima, I., Miyajaki, E., and Yasumori, I., *J. Chem. Soc., Faraday Trans. 1* **80**, 841 (1984).
18. Lapidus, A., Krylova, A., Kazanskii, V., Borovkov, V., Zaitsev, A., Rathousky, J., Zukal, A., and Jancalkova, M., *Appl. Catal.* **73**, 65 (1991).
19. Dees, M. J., Shidi, T., Iwasawa, Y., and Ponec, V., *J. Catal.* **124**, 530 (1990).
20. Heal, M. J., Leisegang, E. C., and Torrington, R. G., *J. Catal.* **51**, 314 (1978).

21. Ishi, S.-I, Ohno, Y., and Viswanathan, B., *Surf. Sci.* **161**, 349 (1985).
22. Kip, B. J., Hermans, E. G. F., Van Wolput, J. H. M. C., Hermans, N. M. A., Van Grondel, J., and Prins, R., *Appl. Catal.* **35**, 109 (1987).
23. Ho, S. W., in preparation.
24. Zowitiak, J. M., and Bartholowew, C. H., *J. Catal.* **83**, 107 (1983).
25. Bridge, M. E., Comrie, C. M., and Lambert, R. M., *J. Catal.* **58**, 28 (1979).
26. Bridge, M. E., Comrie, C. M., and Lambert, R. M., *Surf. Sci.* **67**, 393 (1977).
27. Bardi, U., Tiscione, P., and Rovida, G., *Appl. Surf. Sci.* **27**, 299 (1986).
28. Prior, K. A., Schwaha, K., and Lambert, R. M., *Surf. Sci.* **77**, 193 (1978).
29. Niemela, M. K., Krause, A. O. I., Vaara, T., Kiviaho, J. J., and Reinikainen, M. K. O., *Appl. Catal.* **147**, 325 (1996).
30. Watanabe, M., *J. Catal.* **110**, 37 (1988).
31. Glugla, P. G., Baily, K. M., and Falconer, J. L., *J. Catal.* **115**, 24 (1989).
32. Sen, B., and Falconer, J. L., *J. Catal.* **122**, 68 (1990).
33. Yokomizo, G. H., Louis, C., and Bell, A. T., *J. Catal.* **120**, 15 (1989).
34. Underwood, R. P., and Bell, A. T., *J. Catal.* **109**, 61 (1988).
35. Jen, H. W., Zheng, Y., Shriver, D. F., and Sachtler, W. M. F. H., *J. Catal.* **116**, 361 (1989).
36. Wang, D.-Z., Cheng, X.-P., Huang, Z.-E., Wang, X.-Z., and Peng, S.-Y., *Appl. Catal.* **77**, 109 (1991).
37. Papp, H., *Surf. Sci.* **149**, 460 (1985).
38. Je, Y.-T., and Companion, A. L., *Surf. Sci. Lett.* **271**, L345 (1992).
39. Lamotte, J., and Lavalley, J., *J. Chem. Soc., Faraday Trans. 1* **81**, 215 (1985).
40. Lee, D.-K., Lee, J.-H., and Ihm, S.-K., *Appl. Catal.* **36**, 199 (1988).
41. Lee, W. H., and Bartholomew, C. H., *J. Catal.* **120**, 256 (1989).
42. Reuel, R. C., and Bartholomew, C. H., *J. Catal.* **85**, 78 (1984).
43. Reuel, R. C., and Bartholomew, C. H., *J. Catal.* **85**, 63 (1984).
44. Vannice, M. A., *J. Catal.* **50**, 228 (1977).
45. Ledford, J. S., Houalla, M., Proctor, A., and Hercules, D. M., *J. Catal.* **125**, 554 (1990).